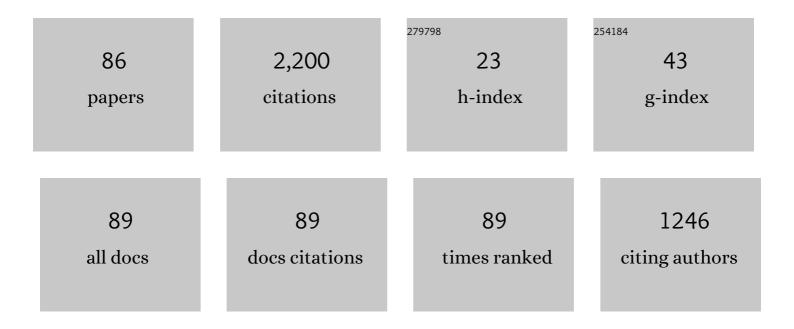
## List of Publications by Year in descending order

Source: https://exaly.com/author-pdf/4622470/publications.pdf Version: 2024-02-01



Cuovulu

#	Article	IF	CITATIONS
1	Effect of freeze-thaw cycles in mechanical behaviors of frozen loess. Cold Regions Science and Technology, 2018, 146, 9-18.	3.5	224
2	Hyperspectral Images Classification With Gabor Filtering and Convolutional Neural Network. IEEE Geoscience and Remote Sensing Letters, 2017, 14, 2355-2359.	3.1	199
3	Multiaxial creep of frozen loess. Mechanics of Materials, 2016, 95, 172-191.	3.2	141
4	Variations in strength and deformation of compacted loess exposed to wetting-drying and freeze-thaw cycles. Cold Regions Science and Technology, 2018, 151, 159-167.	3.5	101
5	Experimental investigation of the path-dependent strength and deformation behaviours of frozen loess. Engineering Geology, 2020, 265, 105449.	6.3	100
6	Influence of Pore Water (Ice) Content on the Strength and Deformability of Frozen Argillaceous Siltstone. Rock Mechanics and Rock Engineering, 2020, 53, 967-974.	5.4	85
7	Investigation of the freeze–thaw states of foundation soils in permafrost areas along the China–Russia Crude Oil Pipeline (CRCOP) route using ground-penetrating radar (GPR). Cold Regions Science and Technology, 2016, 126, 10-21.	3.5	68
8	Effects of freeze-thaw cycle on engineering properties of loess used as road fills in seasonally frozen ground regions, North China. Journal of Mountain Science, 2017, 14, 356-368.	2.0	66
9	Thermal elasto-plastic computation model for a buried oil pipeline in frozen ground. Cold Regions Science and Technology, 2010, 64, 248-255.	3.5	64
10	Pipeline–permafrost interaction monitoring system along the China–Russia crude oil pipeline. Engineering Geology, 2019, 254, 113-125.	6.3	56
11	Permafrost thawing along the China-Russia Crude Oil Pipeline and countermeasures: A case study in Jiagedaqi, Northeast China. Cold Regions Science and Technology, 2018, 155, 308-313.	3.5	50
12	Field observations of cooling performance of thermosyphons on permafrost under the China-Russia Crude Oil Pipeline. Applied Thermal Engineering, 2018, 141, 688-696.	6.0	48
13	Development of freezing–thawing processes of foundation soils surrounding the China–Russia Crude Oil Pipeline in the permafrost areas under a warming climate. Cold Regions Science and Technology, 2010, 64, 226-234.	3.5	45
14	Damage evolution and recrystallization enhancement of frozen loess. International Journal of Damage Mechanics, 2018, 27, 1131-1155.	4.2	44
15	Forecasting the oil temperatures along the proposed China–Russia Crude Oil Pipeline using quasi 3-D transient heat conduction model. Cold Regions Science and Technology, 2010, 64, 235-242.	3.5	40
16	Dynamic responses of frozen subgrade soil exposed to freeze-thaw cycles. Soil Dynamics and Earthquake Engineering, 2022, 152, 107010.	3.8	37
17	Settlement characteristics of unprotected embankment along the Qinghai–Tibet Railway. Cold Regions Science and Technology, 2010, 60, 84-91.	3.5	31
18	Freeze–thaw properties and long-term thermal stability of the unprotected tower foundation soils in permafrost regions along the Qinghai–Tibet Power Transmission Line. Cold Regions Science and Technology, 2016, 121, 258-274.	3.5	31

#	Article	IF	CITATIONS
19	Thermal performance of a combined cooling method of thermosyphons and insulation boards for tower foundation soils along the Qinghai–Tibet Power Transmission Line. Cold Regions Science and Technology, 2016, 121, 226-236.	3.5	30
20	Yield surface evolution for columnar ice. Results in Physics, 2016, 6, 851-859.	4.1	29
21	Experimental study on the dynamic behavior of expansive soil in slopes under freeze-thaw cycles. Cold Regions Science and Technology, 2019, 163, 27-33.	3.5	26
22	Long-term thermal and settlement characteristics of air convection embankments with and without adjacent surface water ponding in permafrost regions. Engineering Geology, 2020, 266, 105464.	6.3	25
23	Thermal Characteristics of the Embankment with Crushed Rock Side Slope to Mitigate Thaw Settlement Hazards of the Qinghaiâ€Tibet Railway. Acta Geologica Sinica, 2009, 83, 1000-1007.	1.4	24
24	LiDAR Data Classification Using Spatial Transformation and CNN. IEEE Geoscience and Remote Sensing Letters, 2019, 16, 125-129.	3.1	23
25	Study on design optimization of a crushed stone layer with shading board placed on a railway embankment on warm permafrost. Cold Regions Science and Technology, 2008, 54, 36-43.	3.5	22
26	Field observation of permafrost degradation under Mo'he airport, Northeastern China from 2007 to 2016. Cold Regions Science and Technology, 2019, 161, 43-50.	3.5	22
27	Early-age hydration heat evolution and kinetics of Portland cement containing nano-silica at different temperatures. Construction and Building Materials, 2022, 334, 127363.	7.2	21
28	Mechanical Properties of Fiber-Reinforced Soil under Triaxial Compression and Parameter Determination Based on the Duncan-Chang Model. Applied Sciences (Switzerland), 2020, 10, 9043.	2.5	20
29	Mass and Heat Balance of a Lake Ice Cover in the Central Asian Arid Climate Zone. Water (Switzerland), 2020, 12, 2888.	2.7	20
30	Globally elevated chemical weathering rates beneath glaciers. Nature Communications, 2022, 13, 407.	12.8	20
31	A strength criterion for frozen clay considering the influence of stress Lode angle. Canadian Geotechnical Journal, 2019, 56, 1557-1572.	2.8	19
32	46-Year (1973–2019) Permafrost Landscape Changes in the Hola Basin, Northeast China Using Machine Learning and Object-Oriented Classification. Remote Sensing, 2021, 13, 1910.	4.0	18
33	A new ripraped-rock slope for high temperature permafrost regions. Cold Regions Science and Technology, 2006, 45, 42-50.	3.5	17
34	Engineering properties of loess stabilized by a type of eco-material, calcium lignosulfonate. Arabian Journal of Geosciences, 2019, 12, 1.	1.3	17
35	A novel evaluation method for accumulative plastic deformation of granular materials subjected to cyclic loading: Taking frozen subgrade soil as an example. Cold Regions Science and Technology, 2020, 179, 103152.	3.5	17
36	Solar radiation transfer for an ice-covered lake in the central Asian arid climate zone. Inland Waters, 2021, 11, 89-103.	2.2	17

#	Article	IF	CITATIONS
37	Thermal state of soils in the active layer and underlain permafrost at the kilometer post 304 site along the China-Russia Crude Oil Pipeline. Journal of Mountain Science, 2016, 13, 1984-1994.	2.0	15
38	Study on the mesostructural evolution mechanism of compacted loess subjected to various weathering actions. Cold Regions Science and Technology, 2019, 167, 102846.	3.5	15
39	Assessment of Freeze–Thaw Hazards and Water Features along the China–Russia Crude Oil Pipeline in Permafrost Regions. Remote Sensing, 2020, 12, 3576.	4.0	15
40	Development of Anisotropy in Sandstone Subjected to Repeated Frost Action. Rock Mechanics and Rock Engineering, 2021, 54, 1863-1874.	5.4	15
41	Permafrost warming along the Mo'he-Jiagedaqi section of the China-Russia crude oil pipeline. Journal of Mountain Science, 2019, 16, 285-295.	2.0	14
42	Grazing exclusion did not affect soil properties in alpine meadows in the Tibetan permafrost region. Ecological Engineering, 2020, 147, 105657.	3.6	14
43	Deformation Monitoring in an Alpine Mining Area in the Tianshan Mountains Based on SBAS-InSAR Technology. Advances in Materials Science and Engineering, 2021, 2021, 1-15.	1.8	14
44	Fracture Mechanical Properties of Frozen Sandstone at Different Initial Saturation Degrees. Rock Mechanics and Rock Engineering, 2022, 55, 3235-3252.	5.4	14
45	Response of bacterial communities to mining activity in the alpine area of the Tianshan Mountain region, China. Environmental Science and Pollution Research, 2021, 28, 15806-15818.	5.3	13
46	Freeze-thaw resistance of eco-material stabilized loess. Journal of Mountain Science, 2021, 18, 794-805.	2.0	13
47	Numerical analysis of frost heave and thawing settlement of the pile–soil system in degraded permafrost region. Environmental Earth Sciences, 2021, 80, 1.	2.7	13
48	SBAS-InSAR-Based Analysis of Surface Deformation in the Eastern Tianshan Mountains, China. Frontiers in Earth Science, 2021, 9, .	1.8	13
49	Quantification of Temporal Decorrelation in X-, C-, and L-Band Interferometry for the Permafrost Region of the Qinghai–Tibet Plateau. IEEE Geoscience and Remote Sensing Letters, 2017, 14, 2285-2289.	3.1	12
50	Study on Tensile Strength and Tensile-Shear Coupling Mechanism of Loess around Lanzhou and Yanan City in China by Unconfined Penetration Test. KSCE Journal of Civil Engineering, 2019, 23, 2471-2482.	1.9	12
51	Effect of Freeze-Thaw Cycles on Mechanical Behavior of Compacted Fine-Grained Soil. , 2012, , .		11
52	Characteristics of the active-layer under the China-Russia Crude Oil pipeline. Journal of Mountain Science, 2021, 18, 323-337.	2.0	11
53	A long-term strength criterion for frozen clay under complex stress states. Cold Regions Science and Technology, 2020, 176, 103089.	3.5	11
54	Porosity of crushed rock layer and its impact on thermal regime of Qinghaiâ^'Tibet Railway embankment. Journal of Central South University, 2017, 24, 977-987.	3.0	10

#	Article	IF	CITATIONS
55	Bioavailable phosphorus distribution in alpine meadow soil is affected by topography in the Tian Shan Mountains. Journal of Mountain Science, 2020, 17, 410-422.	2.0	10
56	Profile distributions of soil organic carbon fractions in a permafrost region of the Qinghai–Tibet Plateau. Permafrost and Periglacial Processes, 2020, 31, 538-547.	3.4	10
57	Preliminary study on cooling effect mechanisms of Qinghai–Tibet railway embankment with open crushed-stone side slope in permafrost regions. Cold Regions Science and Technology, 2006, 45, 193-201.	3.5	9
58	Permafrost warming under the earthen roadbed of the Qinghai–Tibet Railway. Environmental Earth Sciences, 2011, 64, 1975-1983.	2.7	9
59	Laboratory testing on heat transfer of frozen soil blocks used as backfills of pile foundation in permafrost along Qinghai-Tibet electrical transmission line. Arabian Journal of Geosciences, 2015, 8, 2527-2535.	1.3	9
60	Pasture degradation impact on soil carbon and nitrogen fractions of alpine meadow in a Tibetan permafrost region. Journal of Soils and Sediments, 2020, 20, 2330-2342.	3.0	9
61	A novel approach for characterizing frozen soil damage based on mesostructure. International Journal of Damage Mechanics, 2022, 31, 444-463.	4.2	9
62	Effect of Repeated Wetting-Drying-Freezing-Thawing Cycles on the Mechanic Properties and Pore Characteristics of Compacted Loess. Advances in Civil Engineering, 2020, 2020, 1-8.	0.7	8
63	Damage characteristics of the Qinghai-Tibet Highway in permafrost regions based on UAV imagery. International Journal of Pavement Engineering, 2023, 24, .	4.4	8
64	Proposal of a New Method for Controlling the Thaw of Permafrost around the China–Russia Crude Oil Pipeline and a Preliminary Study of Its Ventilation Capacity. Water (Switzerland), 2021, 13, 2908.	2.7	7
65	Damage Properties of the Block-Stone Embankment in the Qinghai–Tibet Highway Using Ground-Penetrating Radar Imagery. Remote Sensing, 2022, 14, 2950.	4.0	7
66	The Outburst of a Lake and Its Impacts on Redistribution of Surface Water Bodies in High-Altitude Permafrost Region. Remote Sensing, 2022, 14, 2918.	4.0	7
67	A novel freezing point determination method for oil–contaminated soils based on electrical resistance measurement and its influencing factors. Science of the Total Environment, 2020, 721, 137821.	8.0	6
68	Automated demarcation of the homogeneous domains of trace distribution within a rock mass based on GLCM and ISODATA. International Journal of Rock Mechanics and Minings Sciences, 2020, 128, 104249.	5.8	5
69	Improving the Mechanical Properties of Red Clay Using Xanthan Gum Biopolymer. International Journal of Polymer Science, 2021, 2021, 1-16.	2.7	5
70	Diurnal Cycle Model of Lake Ice Surface Albedo: A Case Study of Wuliangsuhai Lake. Remote Sensing, 2021, 13, 3334.	4.0	4
71	Three-Dimensional Numerical Investigation on the Seepage Field and Stability of Soil Slope Subjected to Snowmelt Infiltration. Water (Switzerland), 2021, 13, 2729.	2.7	4
72	Controlling factors of soil organic carbon and nitrogen in lucerne grasslands in a semiarid environment. Catena, 2022, 211, 105983.	5.0	4

#	Article	IF	CITATIONS
73	Alternate freezing and thawing enhanced the sediment and nutrient runoff loss in the restored soil of the alpine mining area. Journal of Mountain Science, 0, , 1.	2.0	4
74	Effect of freeze-thaw cycles on the physical and dynamic characteristic of modified Na-bentonite by KCl. Arabian Journal of Geosciences, 2020, 13, 1.	1.3	3
75	Acceleration Frequency Characteristics of the Freight-Train-Induced Vibration of the Beijing-Harbin Railway Subgrade. Shock and Vibration, 2020, 2020, 1-11.	0.6	3
76	Degradation characteristics and bearing capacity model of pile in degraded permafrost. Proceedings of the Institution of Civil Engineers: Geotechnical Engineering, 2022, 175, 414-425.	1.6	2
77	Dynamic Behavior of Geosynthetic-Reinforced Expansive Soil under Freeze-Thaw Cycles. Advances in Civil Engineering, 2021, 2021, 1-11.	0.7	2
78	A 10â€yr thermal regime of permafrost beneath and adjacent to an alpine thermokarst lake, Beiluhe Basin, Qinghai–Tibet Plateau, China. Permafrost and Periglacial Processes, 2021, 32, 618-626.	3.4	1
79	Analysis of Necessity and Feasibility for Ground Improvement in Warm and Ice-Rich Permafrost Regions. Advances in Civil Engineering, 2022, 2022, 1-12.	0.7	1
80	Influence of Warm Oil Pipeline on Underlying Permafrost and Cooling Effect of Thermosyphon Based on Field Observations. Springer Series in Geomechanics and Geoengineering, 2018, , 1424-1428.	0.1	0
81	Experimental Study on Electric Resistivity Characteristics of Compacted Loess under Different Loads and Drying-Wetting Cycles. Advances in Civil Engineering, 2021, 2021, 1-12.	0.7	0
82	Critical Dynamic Stress and Accumulative Deformation Evolution of Embankment Silty Clay Subjected to Cyclic Freeze-Thaw. Shock and Vibration, 2021, 2021, 1-9.	0.6	0
83	Influence of Wetting-Drying Cycle in Road Cut Slope in Loess in Northwest China. Springer Series in Geomechanics and Geoengineering, 2018, , 1508-1511.	0.1	0
84	Centrifuge Model Test on Performance of Thermosyphon Cooled Sandbags Supporting Warm Oil Pipeline Buried in Thawing Permafrost. Springer Series in Geomechanics and Geoengineering, 2018, , 1380-1384.	0.1	0
85	Elastoplastic Model Framework for Saturated Soils Subjected to a Freeze–Thaw Cycle Based on Generalized Plasticity Theory. Materials, 2021, 14, 6485.	2.9	0
86	Experimental Study on the Anisotropy and Non-coaxiality of Frozen Standard Sand under Different Principal Stress Directions. Geofluids, 2022, 2022, 1-15.	0.7	0